Conditional moment method for fully-coupled phase-averaged cavitation models

Spencer H. Bryngelson[a], Tim Colonius[a], Rodney O. Fox[b,c]

[a] Division of Engineering and Applied Science, California Institute of Technology, Pasadena, CA 91125, USA
[b] Department of Chemical and Biological Engineering, Iowa State University, Ames, IA 50011, USA
[c] Center for Multiphase Flow Research and Education, Iowa State University, Ames, IA 50011, USA

Abstract

Eulerian sub-grid models for cavitation like ensemble-averaging are an increasingly viable route for simulating engineering-scale bubbly flow problems. We identify two primary concerns towards enabling physically-faithful simulations: sub-grid model fidelity and computational cost. Previous Euler–Euler models considered the sub-grid bubble radius R and radial velocity $\dot{R}$ to be deterministic and uniform functions of the bubble dynamics model and pressure forcing. We relax this assumption, allowing R and $\dot{R}$ to be arbitrary density functions conditioned on the equilibrium bubble size R_o. Conditional moment inversion methods reconstruct quadrature nodes and weights in the internal coordinate directions, which are used to compute the moments that close the fully-coupled flow equations. We also consider the impact of resolving these disequilibria on quadrature computations in the R_o (polydisperse) coordinate. A one-dimensional acoustically excited bubble screen is used to study the effect of model variations. Results show that resolving R and $\dot{R}$ disequilibria requires only modest computational cost. Variation of their coordinate density functions lead to variations in the dynamic response of the bubble screen, which in principle may be required to faithfully represent actual bubble screens. We also observe increasing smoothness of the bubble screen pressure response with increasing $\dot{R}$ variation and decreasing R variation. Despite this, the cost of resolving the R_o-coordinate quadrature direction is dominated by an intrinsically oscillatory behavior associated with Rayleigh–Plesset-like bubble dynamics rather than the R and $\dot{R}$ distributions.

Keywords: Quadrature moment methods, bubbly flow, cavitation, sub-grid model, phase averaging

1. Introduction

Bubble clouds cavitate in applications of broad engineering interest. Examples include blast trauma [1], kidney stone pulverization lithotripsy [2], and flows over ship propellers and hydrofoils [3]. Realistic simulation of their dynamics and interaction with acoustic waves enables design in these areas. However, scale separations preclude direct numerical simulation of cavitating bubble dispersions: small bubbles nucleate and cavitate rapidly relative to the larger and longer features of suspending flow.

Sub-grid methods address scale chasms via Euler–Euler or Euler–Lagrange phase averaging. Our previous review of phase averaging indicated that Euler–Euler averaging methods can enable simulation of engineering-scale cavitating flows [4]. However, their current forms utilize class-based methods that leave important behaviors unchecked.

Actual bubble dynamics are polydisperse, distributed in their equilibrium bubble size R_o [5, 6]. When this distribution is broad, the average response of the bubbles to pressure fluctuations damps and

*Corresponding author; spencer@caltech.edu

disperses [7, 8]. However, previous studies assumed delta-function equilibrium-centered distributions in the bubble dynamic independent variables, e.g. the bubble radii R and their radial velocities $\dot{R}$. This assumption can only be justified via an accompanying assumption that the bubble dispersion is in hydrodynamic equilibrium for all time and space. Unfortunately, verifying this assumption for actual cavitating bubble clouds is challenging.

As a step toward more realistic simulations, we implement a fully-coupled conditional quadrature moment method for assessing bubble dynamic behavior and computational cost in the face of disequilibrium. Such methods describe the evolving statistics of the bubble dynamics state. It is known that skewness and kurtosis form for sufficiently strong bubble dynamics [9]. Thus, our method is based on the conditional hyperbolic quadrature method of moments (CHyQMOM) [10], which does not *a priori* assume a distribution shape. Our implementation couples CHyQMOM to the compressible flow equations as in Bryngelson et al. [4]. Section 2 details this formulation and the bubble model that closes it.

Bubble disequilibria dynamics can be assessed via a broad change of unit problems. Herein, we consider an acoustically excited bubble screen due to its physical relevance and the availability of reference data [11]. Varying characters of the statistical state of cavitation are controllable via the initial density functions describing their distributions. Here, we vary the breadth of initially log-normal and normal profiles for radial and radial velocity coordinates, respectively. Section 3 details the ability of our method to represent the evolving statistics of fully-polydisperse bubble dynamics and section 4 provides concluding remarks.

2. Model formulation

2.1. Rayleigh–Plesset bubble dynamic model

The bubbles are assumed to be spherical and gas-filled with dynamics governed by a Rayleigh–Plesslet equation for the bubble radius R and its time derivatives (overdots):

$$R\ddot{R} + \frac{3}{2}\dot{R}^2 + \frac{4}{\mathrm{Re}}\frac{\dot{R}}{R} = \left(\frac{R_o}{R}\right)^{3\gamma} - C_p(t), \tag{1}$$

where Re is the Reynolds number (dimensionless ratio of inertial to viscous effects) whose value is chosen as a repsentation of micron-scale bubbles in water. The forcing term $C_p(t) \equiv p_l(t)/p_0$ is the ratio of suspending liquid and atmospheric pressures. The bubble contents compress via a polytropic adiabatic process with coefficient $\gamma = 1.4$.

2.2. Quadrature moment method

A population balance equation (PBE) governs the number density function $f(\boldsymbol{\xi})$ representing the bubble statistics in terms of its internal coordinates $\boldsymbol{\xi} = \{R, \dot{R}, R_o\}$ [12]. Following a usual procedure [12], we describe f via a finite set of raw moments μ_{lmn} where l, m, and n correspond to the R, $\dot{R}$, and R_o coordinate directions. The moment transport equations follow from [9]:

$$\frac{\partial \mu_{lmn}}{\partial t} = l\mu_{l-1,m+1,n} + m\int_{\Omega} \ddot{R}(\boldsymbol{\xi}) R^l \dot{R}^{m-1} R_o^n f(\boldsymbol{\xi})\, \mathrm{d}\boldsymbol{\xi}. \tag{2}$$

Since R_o is not a dynamic variable the total moments can be recast as

$$\mu_{lmn} = \int_{\Omega_{R_o}} f(R_o) R_o^m \mu_{lm}(R_o)\, \mathrm{d}R_o \quad \text{where} \quad \mu_{lm}(R_o) = \int_{\Omega_{R\times\dot{R}}} f(R, \dot{R}|R_o) R^l \dot{R}^m \,\mathrm{d}R \mathrm{d}\dot{R} \tag{3}$$

In (3), $f(R_o)$ is a static log-normal distribution corresponding to polydispersity and $f(R, \dot{R}|R_o)$ are the conditional number density functions. Since $f(R_o)$ is fixed in time, the first integral is computed with a fixed quadrature formula. Conditional moment methods approximate the multi-dimensional moments $\mu_{lm}(R_o)$ [13, 14].

2.3. Averaging

Our formulation of the ensemble-averaged equations generally follows that of Zhang and Prosperetti [15] and Ando [16]. A complete description of them in included in previous works [4]. In brief, they differentiate from the multi-component compressible flow equations by modifying the liquid pressure and volume fraction equations with source terms. These source terms are functions of the raw moments μlmn that are computed using the quadrature rules of section 2.2. The governing equations are solved using the MFC open-source flow solver. It uses a diffuse interface method with fifth-order-accurate WENO reconstruction, a HLLC approximate Riemann solver, and third-order-accurate SSP–RK3 time integration. Further details on the implementation are available elsewhere [17].

3. Results

3.1. Uncoupled bubble dynamics statistics in the R–$\dot{R}$ phase-space

We first assess the ability of CHyQMOM to represent the statistics associated with R_o-monodisperse but R and $\dot{R}$ disequilibrium bubble dynamics. The statistics are initialized with log-normal and normal distributions with variances σ_R^2 and $\sigma_{\dot{R}}^2$ for the R and $\dot{R}$ dynamics, respectively. The bubbles respond to a uniform pressure forcing C_p.

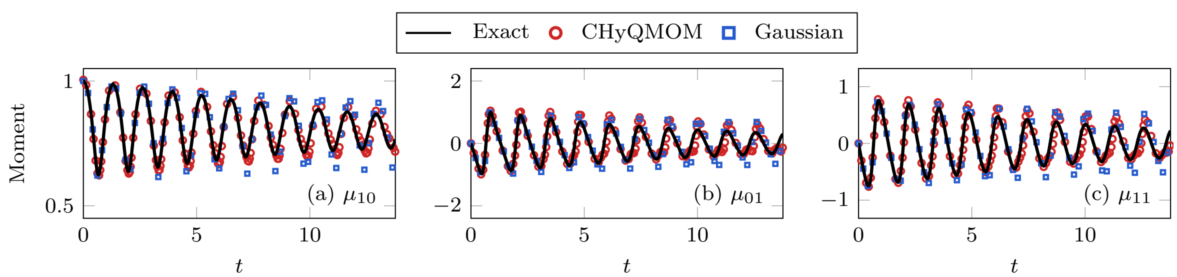

Figure 1: Example moment evolutions as labeled for bubble dynamics parameterized by $R_o = 1$ and $\mathrm{Re} = 10^2$ and dimensionless shape parameters $\sigma_R = \sigma_{\dot{R}} = 0.2$. The CHyQMOM implementation uses two quadrature nodes in each internal coordinate direction. The surrogate exact solution is provided by 10^4 Monte Carlo simulations.

Figure 1 shows the evolution of an example moment set and forcing $C_p = 0.3$, which is known to develop significant skewness and kurtosis [9]. We note that the conclusions drawn from this moment set and pressure ratio is representative of a broader range of C_p and higher-order moments alike. The figure shows that the 4-node CHyQMOM closure is sufficient to accurately represent the moments. The discrete L_2 error for up to second-order moments are smaller for CHyQMOM than Gaussian closure (see [9]). Thus, we move forward CHyQMOM for its ability to efficiently represent the $R - \dot{R}$ statistics.

3.2. Fully-coupled polydisperse bubble screens

We next assess the bubble dynamics and statistics in an acoustically-excited dilute screen region. The bubble screen parameterization generally matches that of Bryngelson et al. [4], with a width of

5 mm and initial void fraction $\alpha_o = 10^{-4}$. The acoustic wave is a single period of a sinusoid with peak amplitude $0.3p_0$ and frequency 300 kHz.

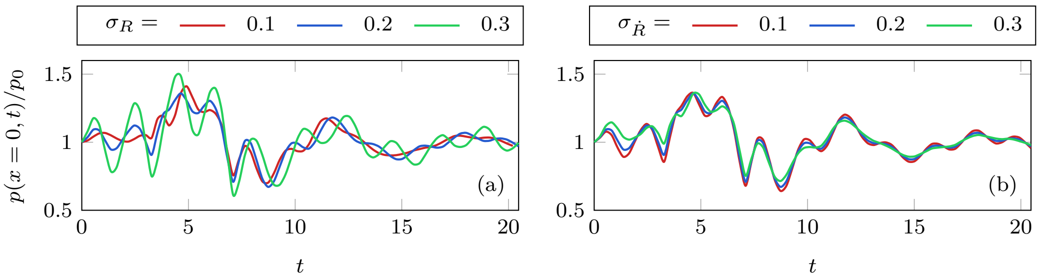

Figure 2: Bubble-screen-centered pressure before, during, and after excitement due to an acoustic wave. The bubbles are polydisperse with log-normal R_o distribution ($\sigma_{R_o} = 0.2$) and $\mathrm{Re} = 10^3$. Panels (a) and (b) show variation in σ_R and $\sigma_{\dot{R}}$, respectively, about a $\sigma_R = \sigma_{\dot{R}} = 0.2$ representative state.

Figure 2 shows the dynamics associated with a bubble screen in varying degrees of statistical disequilibrium. Panel (a) shows a shorter-wavelength oscillatory behavior superimposing the longer acoustic waves. These oscillations are larger in amplitude for larger σ_R. Panel (b) shows that phase-cancellation can result in a smoother pressure profile, with increasingly smooth profiles for larger $\sigma_{\dot{R}}$. Together, behaviors are qualitatively similar to those associated with varying R_o distribution widths. Thus, tuning to an anticipated R_o distribution based upon just single-probe pressure measurements may not be sufficient.

In the results of figure 2, Simpson's rule with 61 nodes closes the moment system in the R_o internal coordinate, Thus, the primary computational cost of these simulations is associated with the R_o-polydispersity, rather than the four-node CHyQMOM $R - \dot{R}$ closure. Further, resolving the R_o dynamics is relatively insensitive to both the type of quadrature used in that direction (e.g. Gaussian-type quadratures) and the R and $\dot{R}$ distributions. As a result, analyzing the effect of R and $\dot{R}$ disequilibria on more complex cavitating flows should not be prohibitive.

4. Conclusion

We introduced a fully-coupled numerical method for simulating sub-grid cavitating bubble dispersions in full statistical disequilibrium. Our results showed that only few quadrature points are required to represent the statistics of the bubble dynamic variables when the population has one equilibrium radius. Modeling for this disequilibrium results in a qualitatively different pressure response of an excited bubble screen. Thus, modeling R–$\dot{R}$ disequilibria and statistics might be necessary for representing actual cavitating bubble dispersions. Detailed experimental data are required to determine if this is indeed required in some or all cases. Further, our results indicated that phase-cancellation can modestly reduce some computational costs associated with resolving the R_o coordinate. However, R_o-direction quadrature costs still dominate the solution of broadly polydisperse bubble populations. This leaves the door open for new approaches to reduce computational cost of R_o-polydispersity.

Acknowledgements

The US Office of Naval Research supported this work under grant numbers N0014-17-1-2676 and N0014-18-1-2625.

References

[1] K. Laksari, S. Assari, B. Seibold, K. Sadeghipour, K. Darvish, Computational simulation of the mechanical response of brain tissue under blast loading, Biomech. Model. Mechanobiol. 14 (2015) 459–472.

[2] K. Maeda, T. Colonius, Bubble cloud dynamics in an ultrasound field, J. Fluid Mech. 862 (2019) 1105–1134.

[3] P. A. Chang, M. Ebert, Y. L. Young, Z. Liu, K. Mahesh, H. Jang, M. Shearer, Propeller forces and structural response due to crashback, in: 27th Symposium on Naval Hydrodynamics, 2008.

[4] S. H. Bryngelson, K. Schmidmayer, T. Colonius, A quantitative comparison of phase-averaged models for bubbly, cavitating flows, Int. J. Mult. Flow 115 (2019) 137–143.

[5] M. Vanni, Approximate population balance equations for aggregation breakage processes, J. Colloid Interface Sci. 221 (2000) 143–160.

[6] K. Ando, T. Colonius, C. E. Brennen, Numerical simulation of shock propagation in a polydisperse bubbly liquid, Int. J. Mult. Flow 37 (2011) 596–608.

[7] P. Smereka, A Vlasov equation for pressure wave propagation in bubbly fluids, J. Fluid Mech. 454 (2002) 287–325.

[8] T. Colonius, R. Hagmeijer, K. Ando, C. E. Brennen, Statistical equilibrium of bubble oscillations in dilute bubbly flows, Phys. Fluids 20 (2008).

[9] S. H. Bryngelson, A. Charalampopoulos, T. P. Sapsis, T. Colonius, A Gaussian moment method and its augmentation via LSTM recurrent neural networks for the statistics of cavitating bubble populations, Int. J. Multiph. Flow 127 (2020) 103262.

[10] R. O. Fox, F. Laurent, A. Vié, Conditional hyperbolic quadrature method of moments for kinetic equations, J. Comput. Phys. 365 (2018) 269–293.

[11] S. N. Domenico, Acoustic wave propagation in air-bubble curtains in water–Part I: History and theory, Geophysics 47 (1982) 345–353.

[12] R. O. Fox, Computational models for turbulent reacting flows, Cambridge University Press, 2003.

[13] C. Yuan, R. O. Fox, Conditional quadrature method of moments for kinetic equations, J. Comput. Phys. 230 (2011) 8216–8246.

[14] R. G. Patel, O. Desjardins, R. O. Fox, Three-dimensional conditional hyperbolic quadrature method of moments, J. Comp. Phys. X 1 (2019) 100006.

[15] D. Z. Zhang, A. Prosperetti, Ensemble phase-averaged equations for bubbly flows, Phys. Fluids 6 (1994).

[16] K. Ando, Effects of polydispersity in bubbly flows, Ph.D. thesis, California Institute of Technology, 2010.

[17] S. H. Bryngelson, K. Schmidmayer, V. Coralic, J. C. Meng, K. Maeda, T. Colonius, MFC: An open-source high-order multi-component, multi-phase, and multi-scale compressible flow solver, Comp. Phys. Comm. (2020) 107396.